Supplementary Figures

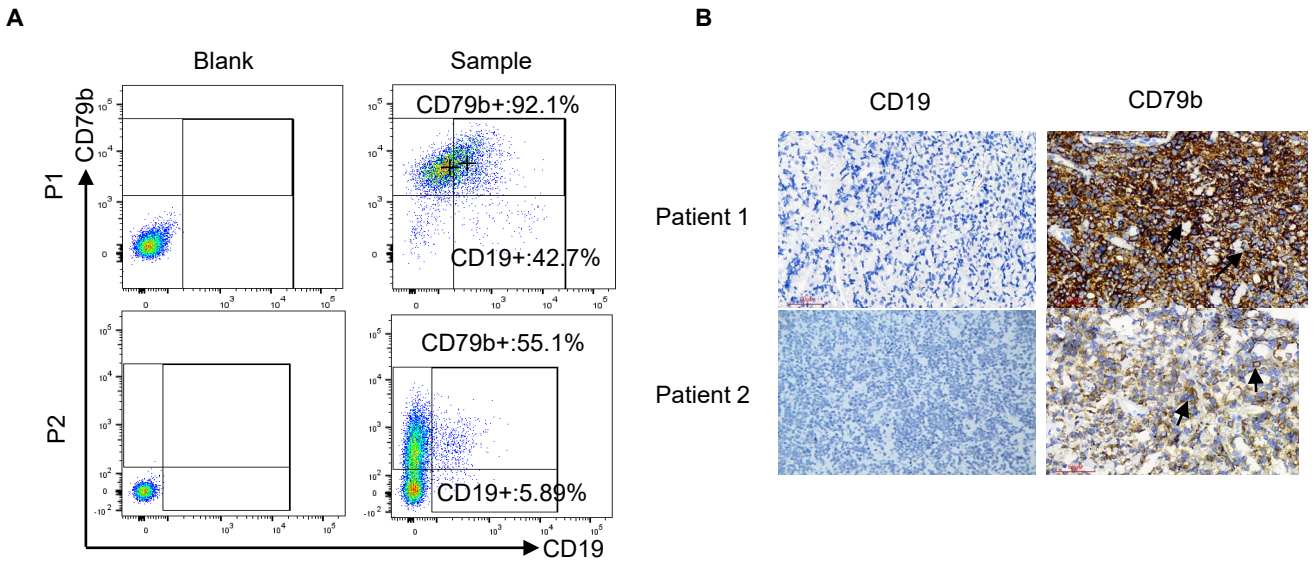

Figure S1. The expression of CD19 and CD79b in B-cell lymphoma samples.

(A) Flow cytometric analysis of CD79b and CD19 expressions on primary tumor cells; P1, DLBCL patient, tumor cells were isolated from ascites; P2, PMBL (primary mediastinal large B-cell lymphoma) patient, tumor cells were isolated from pleural fluid; Sample without staining was indicated as blank. **(B)** Immunohistochemistry images of CD19 and CD79b in tumor tissues from B-cell lymphoma patients after CAR-19 T therapy.

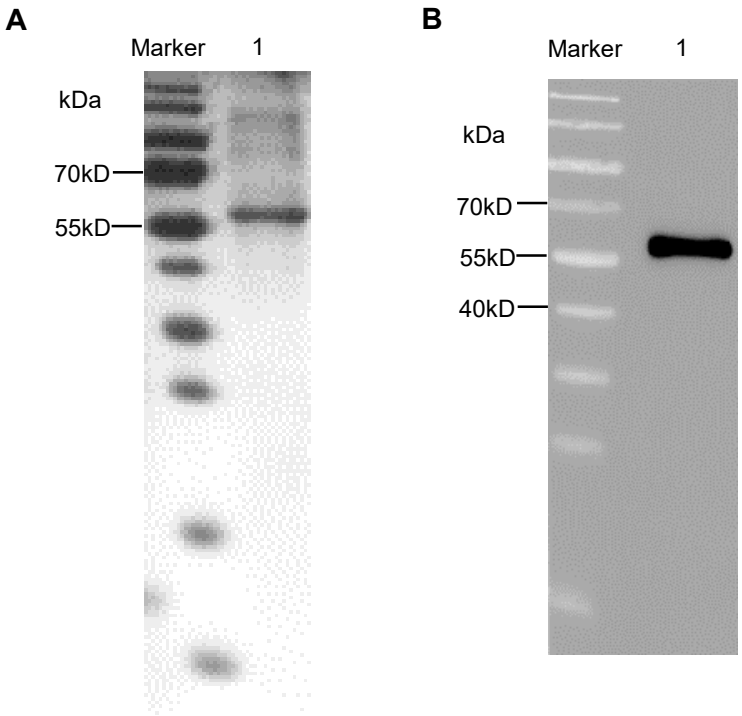

Figure S2. SDS-PAGE and Western blot analyses of BV28-OKT3

(A) SDS-PAGE analysis of BV28-OKT3; **(B)** Western blot analysis of BV28-OKT3.

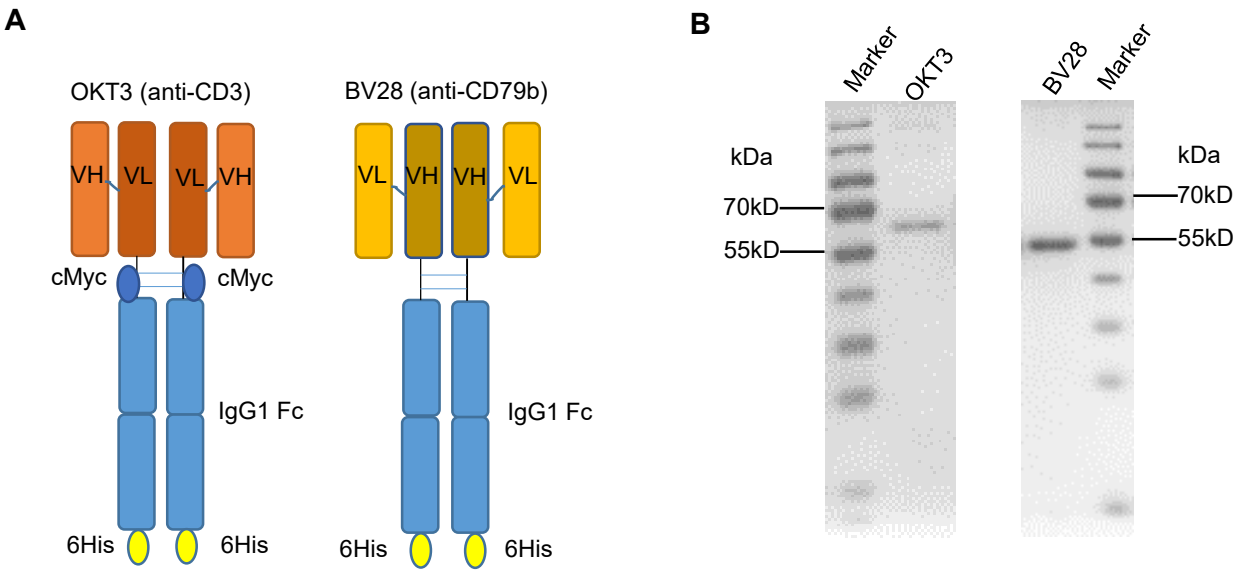

FigureS3. Production of OKT3 and BV28 antibody. (A) Structure of OKT3 (Left) and BV28 (Right); **(B)** SDS-PAGE analysis of the purified OKT3 (Left) and BV28 (Right).

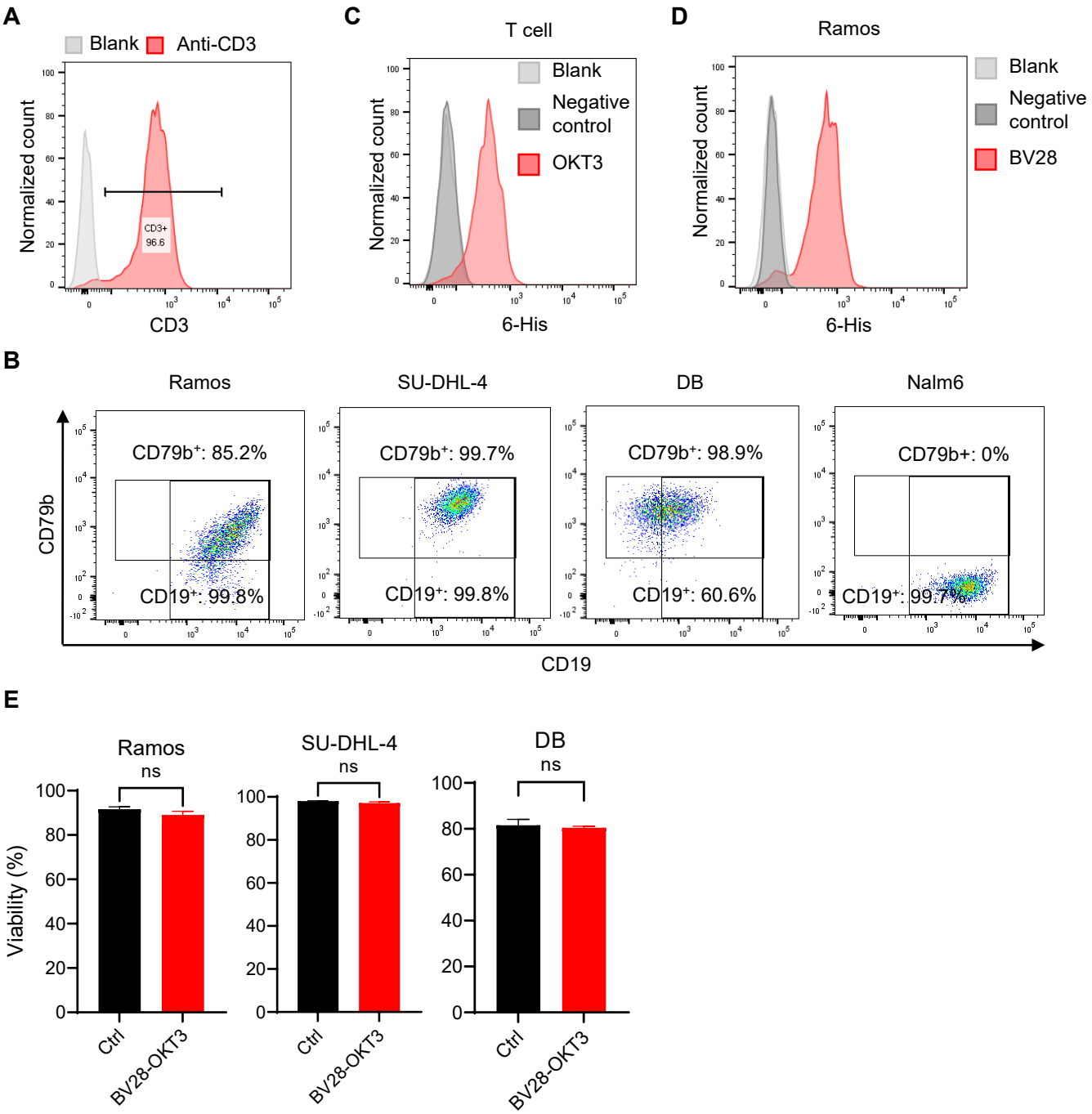

Figure S4. The binding ability of OKT3 and BV28 with T cells and lymphoma cells.

(A) Flow cytometric analysis of CD3 expression in PBMCs after stimulation for 48 h. **(B)** Flow cytometric analysis of CD19 and CD79b expressions on Ramos, SU-DHL-4, DB, and Nalm6 cell lines. **(C)** Flow cytometric analysis of the binding capability of OKT3 to T cells. **(D)** Flow cytometric analysis of the binding capability of BV28 to Ramos. Samples without staining were indicated as blank, and negative controls were cells incubated only with anti-6 His tag antibody; **(E)** Flow cytometric analysis of lymphoma cell line viability ($Dapi^{-}$) in the presence of PBS or 10 μg/mL BV28-OKT3. Ctrl indicated PBS group.

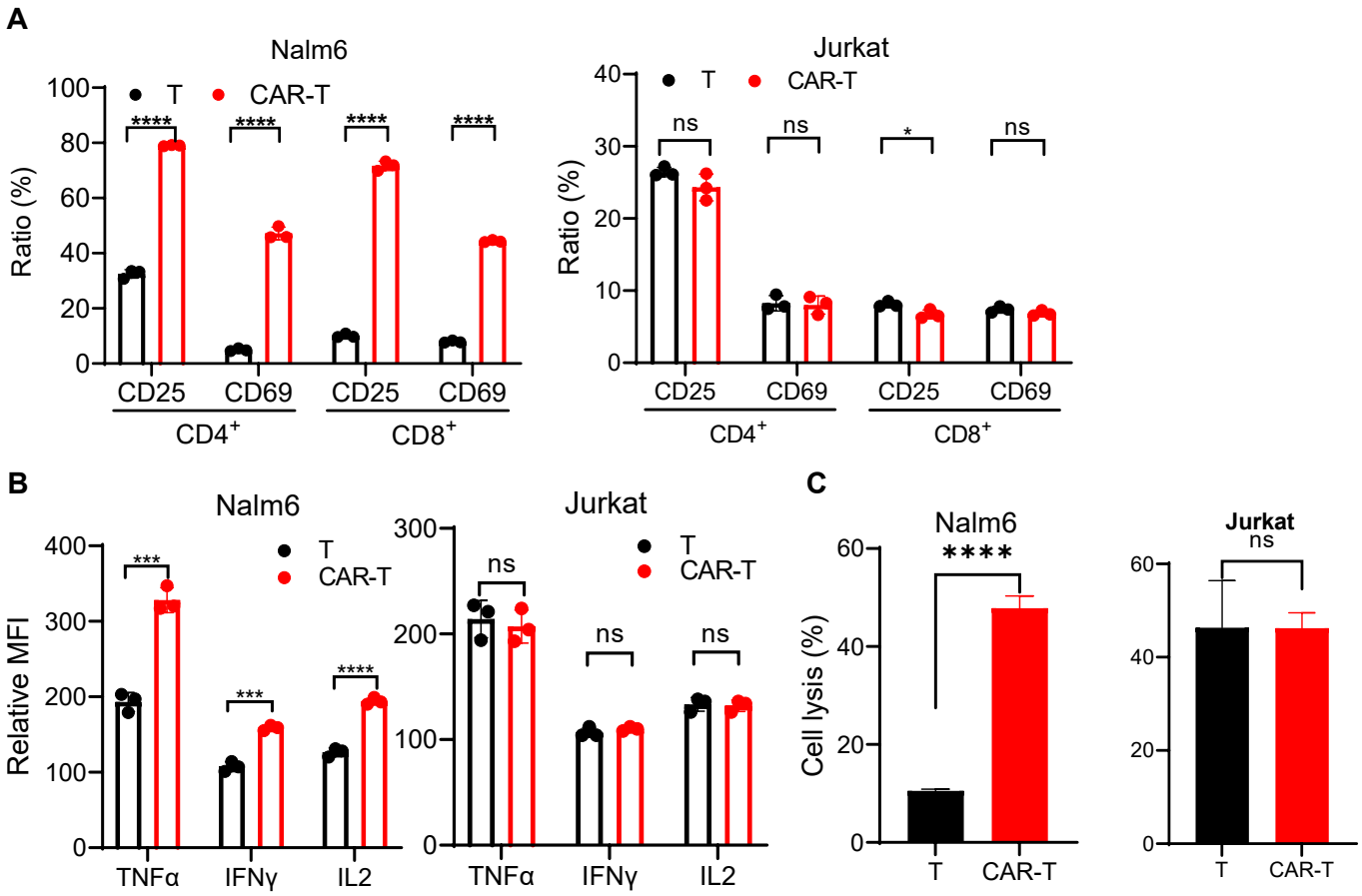

Figure S5. The activity of CAR19-T cells in the present of Nalm6 and Jurkat cells.

(A) Nalm6 and Jurkat cells were co-cultured with equal numbers of T or CAR19-T cells for 24 h. Flow cytometric analysis of $CD25^+$ or $CD69^+$ cell ratios of $CD4^+$ and $CD8^+$ cells. **(B)** Nalm6 or Jurkat cells were co-cultured with equal numbers of T or CAR19-T cells for 18 h. After the addition of transport protein inhibition, these cells were then cultured continuously for another 6 h. The mean fluorescence intensity of TNFα, IFNγ, and IL2 of T or CAR19-T cells was tested by FMC. **(C)** CFSE-labeled Nalm6 and Jurkat cells were co-cultured with equal numbers of T or CAR19-T cells for 24 h. Flow cytometric analysis of cell lysis ratios of Nalm6 and Jurkat cells.

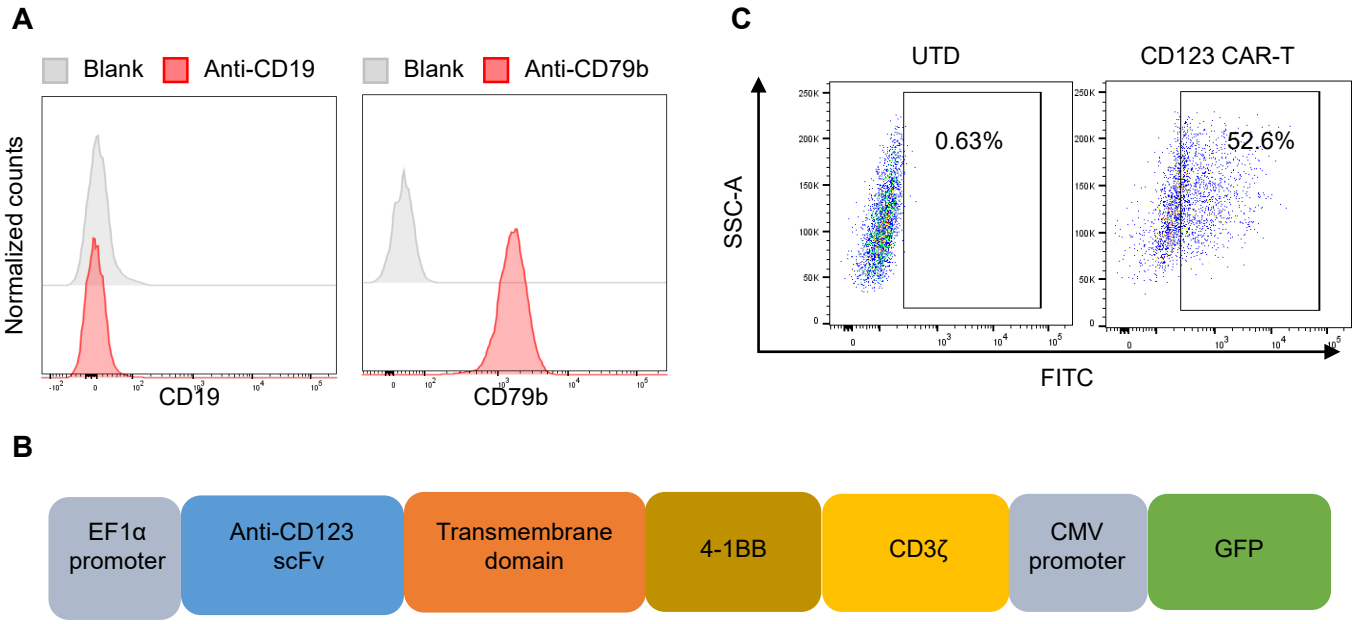

Figure S6. Construction of CD123 CAR-T cells.

(A) Flow cytometric analysis of CD19 and CD79b expressions of CD19-KO SU-DHL-4. Blank indicated samples without staining. **(B)** Structure of CAR123. **(C)** GFP expression in CAR123-T cells was assessed using flow cytometry. UTD indicated untransduced T cells.

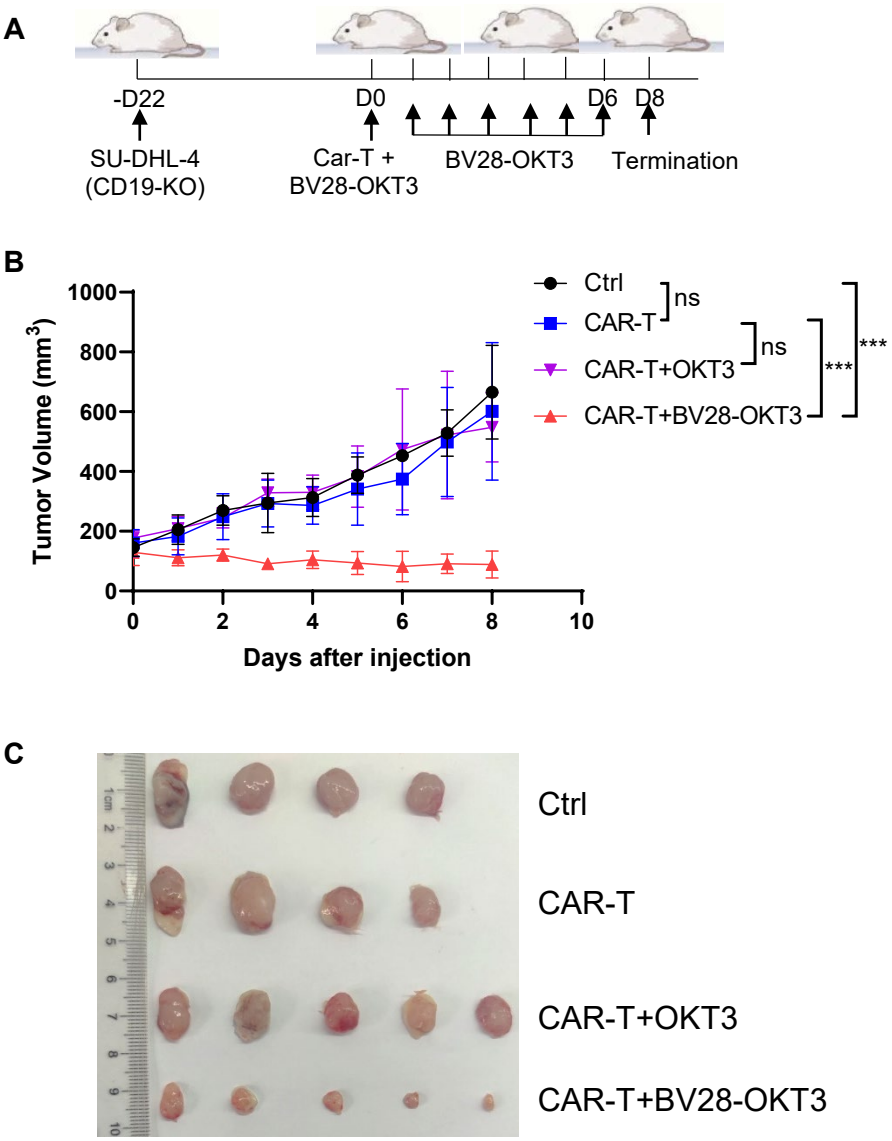

Figure S7. BV28-OKT3 overcomes CD19 antigen escape *in vivo*.

(A) Schematic representation depicts the xenograft mouse model. NSG mice were subcutaneously injected with 1 × 10^7 CD19-KO SU-DHL-4 cells. When tumors reached a volume of approximately 100 mm^3, mice were randomized into four groups and received different treatments: Control group (n = 4), CAR-T group (n = 4), CAR-T + OKT3 group (n = 5), CAR-T + BV28-OKT3 group (n = 5); **(B)** Tumor growth curves of all mice were shown (means ± SD). One-way ANOVA was used for analysis at D8. *, $P < 0.05$; **, $P < 0.01$; ***, $P < 0.001$ **(C)** Images of the tumors harvested from the mice at the end of the experiment.

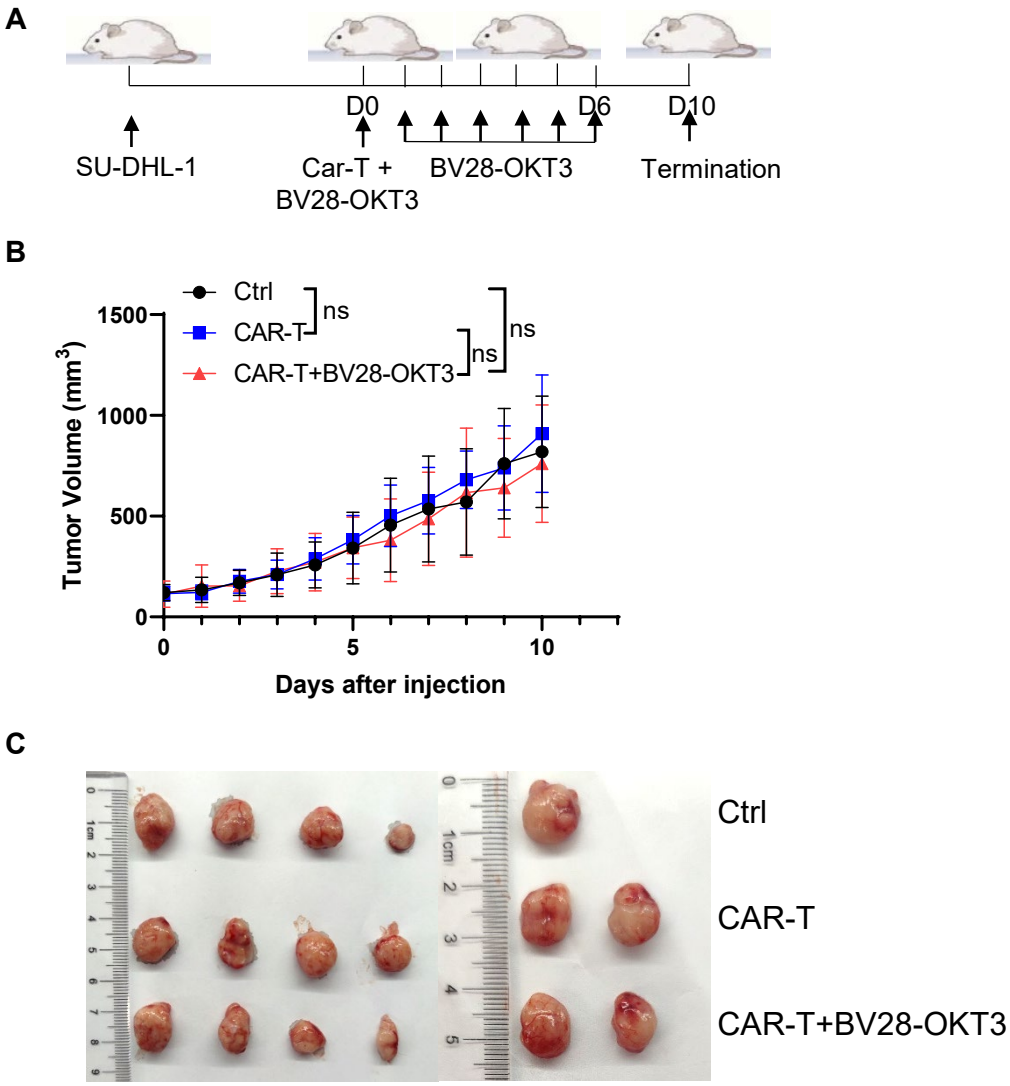

Figure S8. BV28-OKT3 inhibited tumor growth *in vivo* depended on CD79b.

(A) Schematic representation depicts the xenograft mouse model. NSG mice were subcutaneously injected with 5 × 10^6 SU-DHL-1 cells. When tumors reached a volume of approximately 100 mm^3, mice were randomized into three groups and received different treatments: Control group (n = 5), CAR-T group (n = 6), CAR-T + BV28-OKT3 group (n = 6); **(B)** Tumor growth curves of all mice were shown (means ± SD). One-way ANOVA was used for analysis at D10; **(C)** Image of the tumors harvested from the mice at the end of the experiment.

A

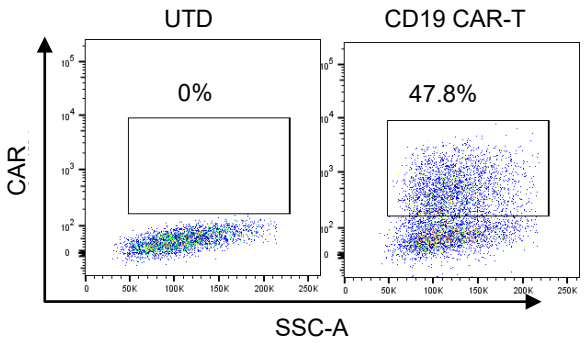

Figure S9. CAR expression level.

(A) The expression levels of CAR were analyzed by flow cytometry.

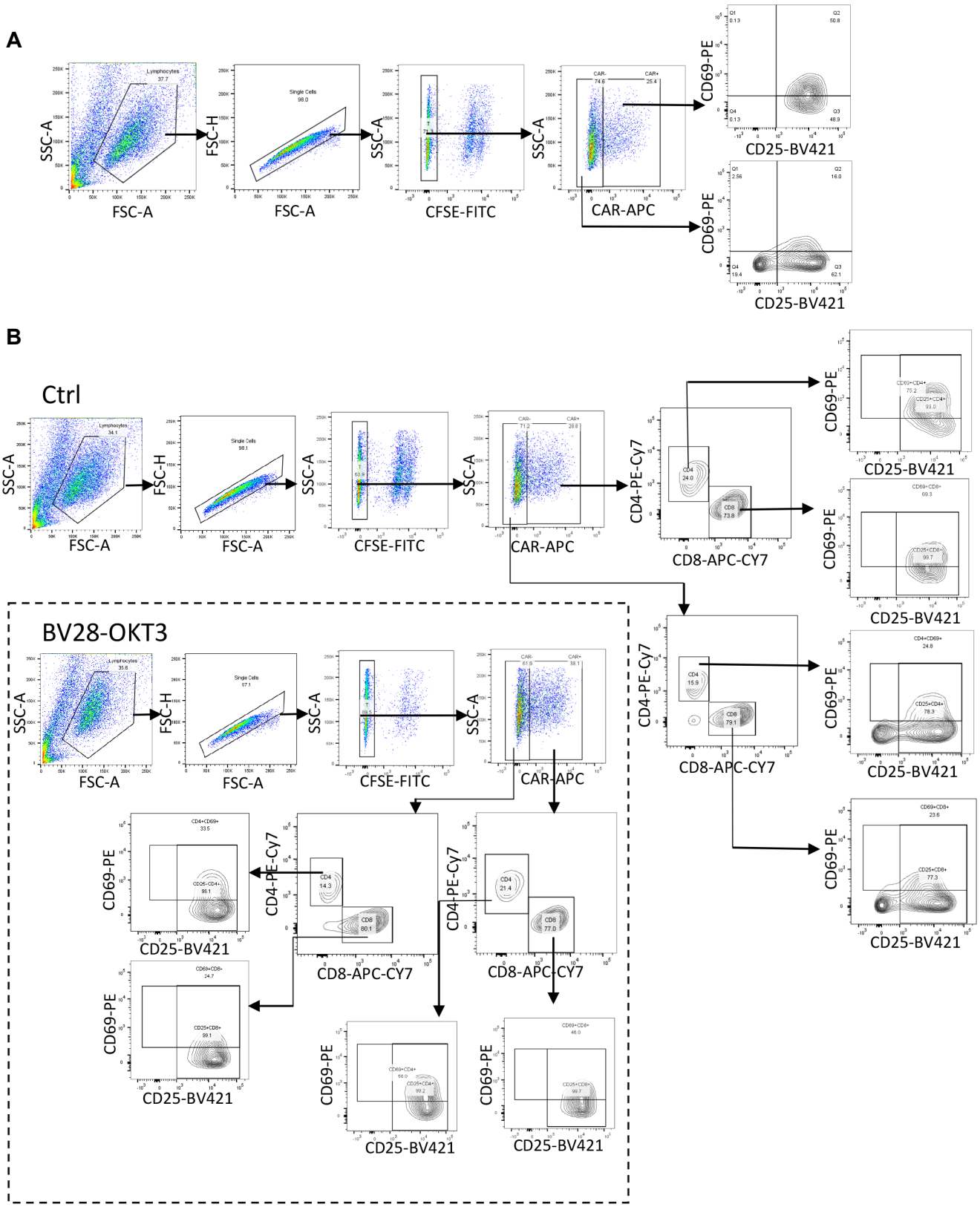

Figure S10. Gating strategies of flow cytometry.

(A) Gating strategies of Fig 6B. **(B)** Gating strategies of Fig 6C. Images out of the dotted box indicated the control group, whereas those in the dotted box indicated BV28-OKT3 group.

A

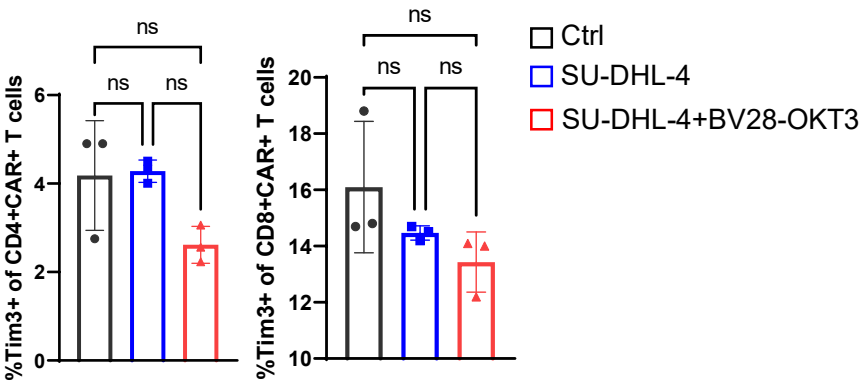

Figure S11. The exhausted level of CAR-T cells

(A) CAR19-T cells were co-cultured with SU-DHL-4 at E:T as 1:1 for 24 h with or without 100 ng/mL BV28-OKT3. Ctrl indicated CAR19-T cells co-cultured with nothing. The expression of Tim3 were accessed by flow cytometry. One-way ANOVA was used for analysis.

*, P < 0.05; **, P < 0.01, ****, P < 0.0001; *****, P < 0.00001;

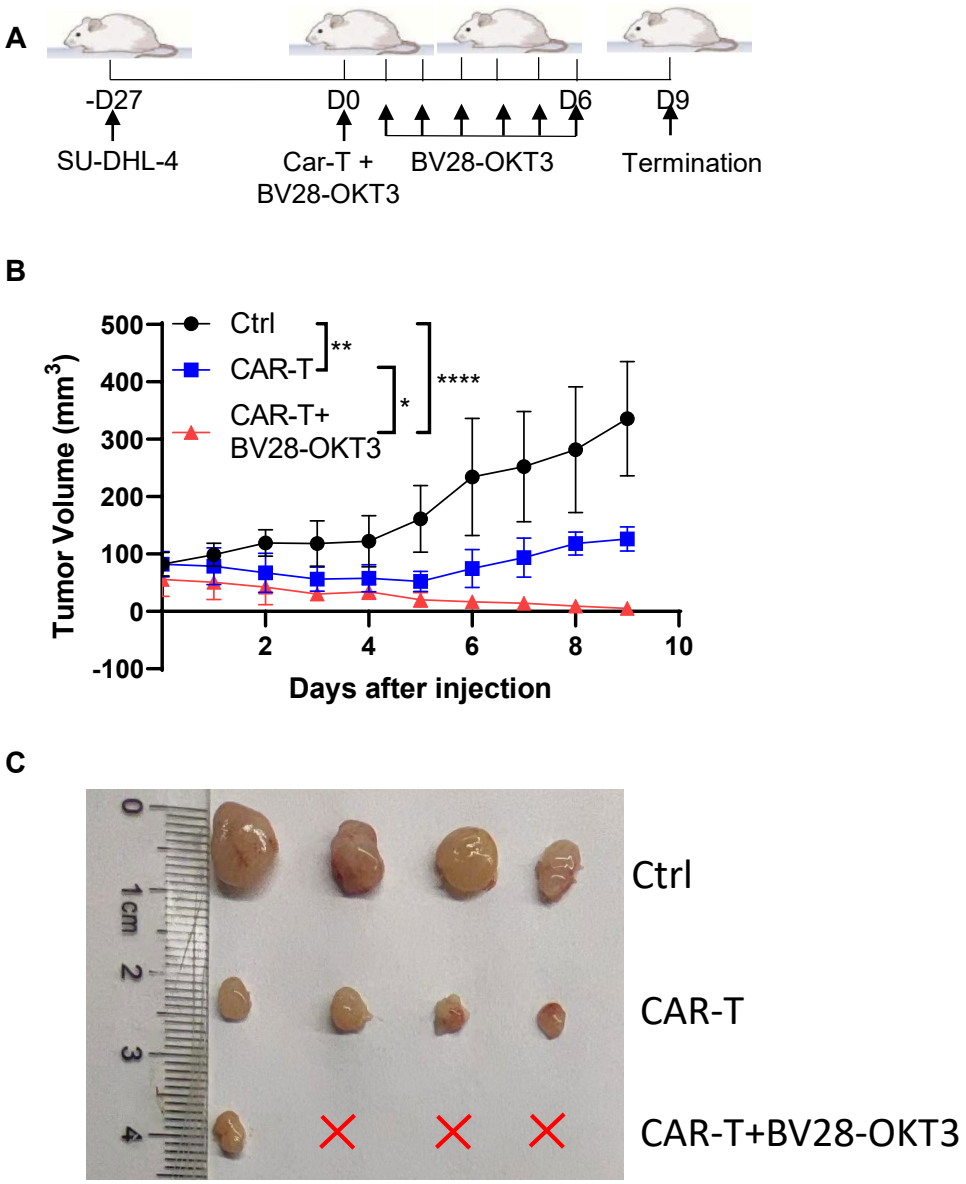

Figure S12. BV28-OKT3 promotes antitumor effects of bystander T cells *in vivo* .
(A) Schematic representation depicts the xenograft mouse model. NSG mice were subcutaneously injected with 1 × 10^7 SU-DHL-4 cells. When tumors reached a volume of approximately 100 mm^3, mice were randomized into three groups and received different treatments: Control group (n = 4), CAR-T group (n = 4), CAR-T + BV28-OKT3 group (n = 4); (B) Tumor growth curves of all mice were shown (means ± SD). One-way ANOVA was used for analysis at D9. *, P < 0.05; **, P < 0.01, ****, P < 0.0001; (C) Images of the tumors harvested from the mice at the end of the experiment, where red x denotes the disappearance of tumor.

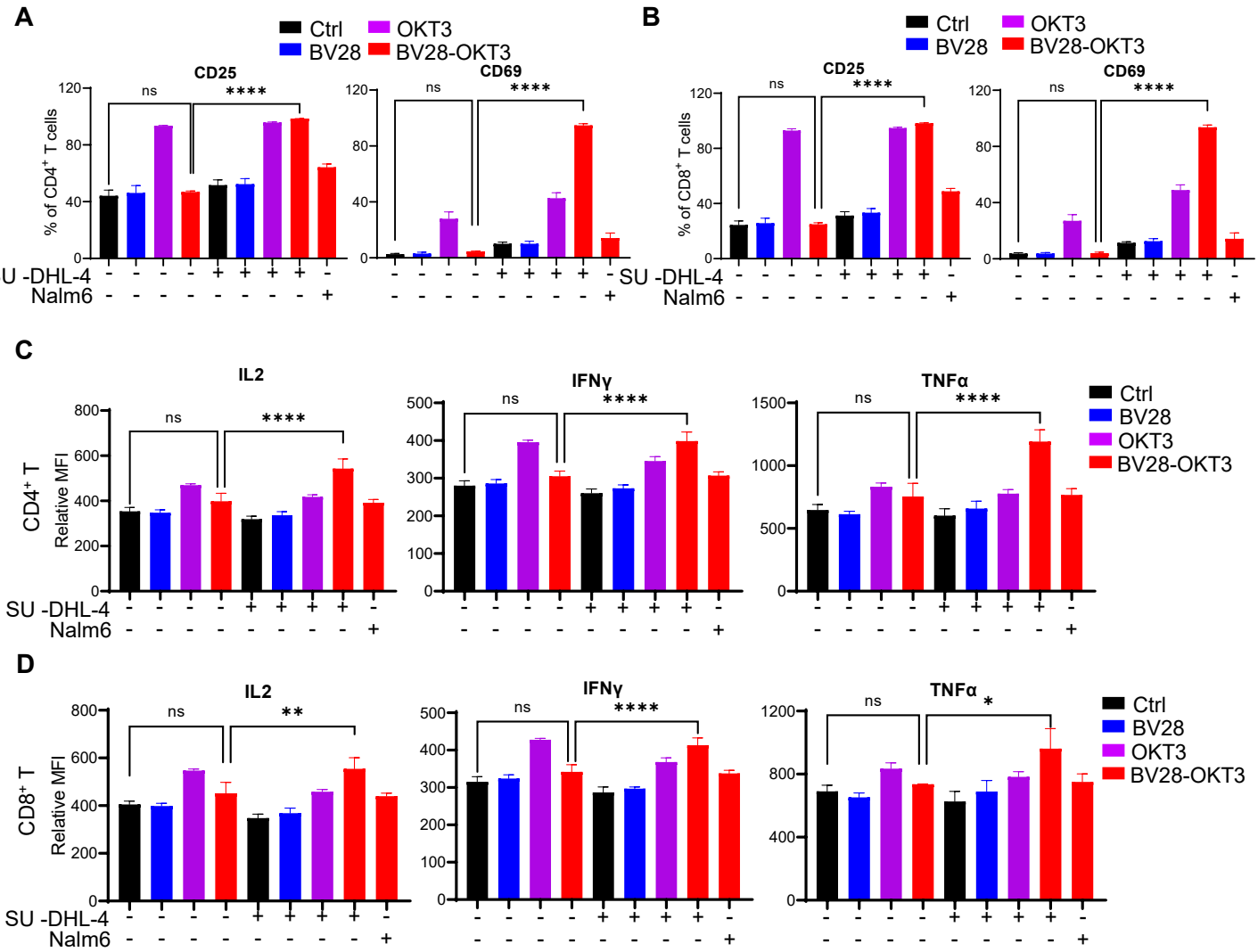

Figure S13. BV28-OKT3-mediated T cell activation depends on the presence of tumor cells.

(A–D) T cells were incubated with equal numbers of SU-DHL-4 or Nalm6 cells, with or without 50 ng/mL BV28-OKT3, OKT3, or BV28 for 24 h; PBS as control. CD25 and CD69 expressions on $CD4^+$ T cells (A) and $CD8^+$ T cells (B), respectively, were assessed by flow cytometry analysis. After incubation for 18 h, GolgiStop was added into the mix, and the mean fluorescence intensity of IFNγ, TNFβ, and IL2 in $CD4^+$ T cells (C) and $CD8^+$ T cells (D) were assessed by flow cytometry analysis after 6 h.

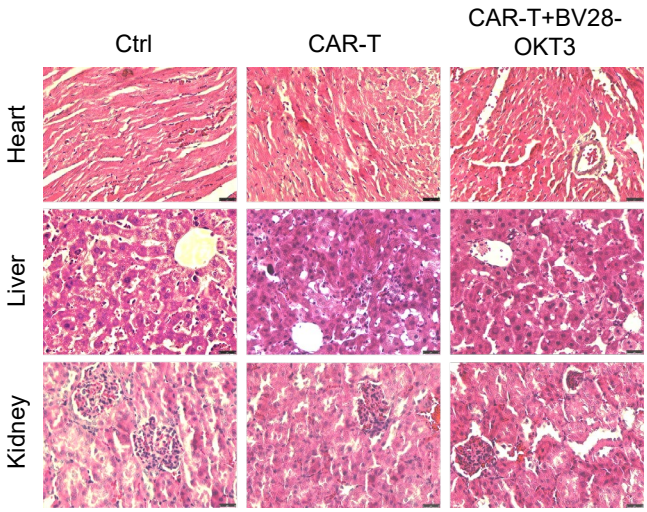

Figure S14. HE staining of Heart, liver, and kidney in Figure 7.

Supplementaty Materials and Methods

Construction of CD19-KO SU-DHL-4 cell lines

SgRNA sequence targeting human CD19 (Personal Biotechnology Co., Ltd., Shanghai, China) was cloned into the LentiCRISPRv2 vector with BsmBI restriction enzyme. LentiCRISPRv2 with CD19 sgRNA, psPAX2, and pMD2.G were then co-transfected to HEK293 cells. Virus particles were collected after 48 and 72 h. SU-DHL-4 cells were transfected with virus, and puromycin was added to select transfected cells after 48 h. CD19-negative cells were chosen by flow cytometry sorting 10–14 days after selection.

SgRNA sequence was as follows: CAGGCCCGAGGAACCTCTAG

Construction of recombinant plasmid

The eukaryotic plasmid pSB-BV28-OKT3-cMyc-His was constructed as follows:

The BV28 and OKT3 fragments were individually amplified from plasmids synthesized from Personal Biotechnology Co., Ltd. (Shanghai, China). The primers were as follows:

BV28 fragment:

F: 5'-CTATTTCCGGTGAATTCCTCGAGGCCACCATGGAGGCCCCCGCCCAGCTGCTGTTCC -3';

R: 5'-GCTGCCGCCGCCGCCGCTGCTCACGGTCACCAGGGTGCCCTG -3';

OKT3 fragment:

F: 5'- AGCGGCGGCGGCGGCAGCGACATCAAGCTGCAGCAGAGCGGCGC-3'

R: 5'-GGAGGGAGAGGGGCGGGATCCTTAGTGGTGGTGGTGGTGGTGGCTGCC-3';

The pSB vector was maintained in the laboratory and digested using *Xho*I and *BamH*I restriction enzymes (NEB, USA). BV28 and OKT3 fragments were then cloned into pSB vector using a Ready-to-Use Seamless Cloning Kit

(Sangon Biotech Co., Ltd., Shanghai, China) to construct pSB-BV28-OKT3-cMyc-His.

Similarly, the eukaryotic plasmid pSB-OKT3-scfv-IgG1 Fc and pSB-BV28-scfv-IgG1 Fc were constructed as follows:

OKT3-scFv and BV28-scfv fragments were individually amplified from plasmids synthesized from Personal Biotechnology Co., Ltd. (Shanghai, China). IgG1 Fc fragment was amplified from the plasmid preserved in the laboratory. The primers were as follows:

OKT3-scFv fragment:

F1: 5'-CTATTTCCGGTGAATTCCTCGAGGCCACCATGGAGGCCCCAGCTCAGCTGCTGTTCCTGCTGCTG-3'

F2: 5'- CTGTGGCTGCCAGACACCACAGGAATGGACATCAAGCTGCAGCAGAGCGG-3'

R: 5'- GCATGTGTGAGTTTTGTCGCCGCTGCTGCCCAGGTCCTCCTCGCTGATCAG-3'

BV28-scfv fragment:

F: 5'-CTATTTCCGGTGAATTCCTCGAGGCCACCATGGAGGCCCCCGCCCAGCTGCTGTTCC -3'

R: 5'-GCATGTGTGAGTTTTGTCGCCGCCGCTGCTCACGGTCACCAGGGTGCCC -3'

IgG1 Fc fragment:

F: 5'-GACAAAACTCACACATGCCCACCGTG-3'

R: 5'-GGAGGGAGAGGGGCGGGATCCTTAGTGATGGTGATGGTGATGTTTACC-3'

OKT3-scfv and BV28-scfv fragments were also individually cloned into digested pSB with IgG1 Fc fragment to construct pSB-OKT3-scfv-IgG1 Fc and pSB-BV28-scfv-IgG1 Fc, respectively.

Sodium dodecyl sulfate-polyacrylamide gel electrophoresis (SDS-PAGE)

SDS-PAGE was conducted on a 12% gel and then stained with 1× coomassie brilliant blue solution for 1 h. The

gel was decolorized with decolorized solution (10% absolute ethanol and 10% glacial acetic acid in ddH_2O) overnight after staining. A Tanon-3500 gel imaging system was used for the imaging.

Flow cytometry

The following antibodies were used to stain cells: APC-conjugated anti-human CD19 antibody (17-0199-42, eBioscience, USA), PE-conjugated CD79b (341404, Biolegend, USA) , APC ef780 -conjugated anti-human CD3 antibody (47-0038-41,eBioscience,USA) , BV28-OKT3, OKT3-scFv-IgG Fc, or BV28-scFv-IgG Fc, CFSE, anti-human CD19 APC antibody (17-0199-42, eBioscience, USA), Alexa Fluor 647-conjugated rabbit anti-FMC63 scFv monoclonal antibody (200102, BioSwan, China), PE/Cy7-conjugated anti-human CD4 antibody (317414, Biolegend, USA), APC ef780-conjugated anti-human CD8 antibody (47-0087-42, eBioscience, USA), BV421-conjugated anti-human CD25 (562442, BD Biosciences, USA) and PE-conjugated anti-human CD69 antibody (310906, Biogend, USA). APC conjugated anti-6 his tag antibody (ab72579, Abcam, UK) was used as a secondary antibody. DAPI was used to label dead cells.

For intracellular cytokine staining, cells were cultured for 18 h, transport protein inhibition (554724, BD, USA) was added, and the cells were cultured continuously for another 6 h. The cells were stained with anti-human CD4, anti-human CD8, and anti-FMC63 scFv antibodies .Next, cells were fixed and permeabilized by the foxp3 transcription factor staining buffer set (00-5523-00, Invitrogen, USA). Finally, cells were stained with Pacific blue-conjugated anti-human IFNγ antibody (502522, Biolegend, USA), PE conjugated anti-human TNFα (12-7349-82, Invitrogen, USA) and FITC-conjugated anti-human IL-2 antibody (11-7029-81, Invitrogen, USA).

To confirm that BV28-OKT3 could bind with T cells, BV28-OKT3 was conjugated with FITC fluorescein by FITC conjugation kit (Sangon Biotech, Shanghai, China) and then were incubated with T cells.

Flow cytometry was performed on a BD FACS Canto Plus flow cytometer, and data were analyzed using FlowJo

V10.

LDH cytotoxicity assay

LDH （Lactatedehydrogenase） cytotoxicity assay kit (C1007, Beyotime, Shanghai, China) was used to test cytotoxicity. Briefly, 1 × 105 target and 1 × 105 effect cells were incubated with or without BV28-OKT3 or control antibodies in a 96-well round-bottom culture plate for 24 h. The 96-well plate was then centrifuged at 320 g for 5 min. The supernatant (120 μL) was removed from each well and placed into a new 96-well flat plate, followed by the addition of 60 μL/well of the reaction solution and incubation for 30 min. Subsequently, the absorbance was measured at 490 nm to calculate cytotoxicity.

Immunofluorescence (IF)

Tumor tissues were fixed in 4% paraformaldehyde (PFA) (Beyotime, Shanghai, China) overnight and then incubated in 20% sucrose for 48 h for dehydration. The tissues were embedded in O.C.T., and frozen sections were finally obtained. Sections were permeabilized in 0.5% Triton-X100 for 15 min. A total of 20% goat serum was used to block sections for 1 h. Anti-human CD8 (300908, 1:100, Biolegend, USA) or anti-human CD3 antibody (11-0039042, BD Biosciences, USA) was diluted and incubated with sections overnight at 4 ℃. The sections were then washed with PBS three times and incubated with DAPI for 5 min. After washing three times, antifade mounting medium was added and images were acquired using a confocal microscope.

Histology imaging

Briefly, heart, kidney, and heart tissues were fixed in 4% PFA for 24 h. After dehydration, tissues were then paraffin-embedded, sectioned, and subsequently stained with hematoxylin and eosin. Finally, tissue sections were observed using a microscope (Leica, Germany).

Immunohistochemistry

Immunohistochemistry images of patients were provided by Tongji Hospital.

Supplementary text: Amino acid sequences of antibodies

1. BV28-OKT3-cMyc-His:

MEAPAQLLFLLLLWLPDTTGDIQLTQSPSSLSASVGDRVTITCKASQSVDYEGDSFLNWYQQKPGK
APKLLIYAASNLESGVPSRFSGSGSGTDFTLTISSLQPEDFATYYCQQSNEDPLTFGQGTKVEIKRGGG
GSGGGGSGGGGSEVQLVESGGGLVQPGGSLRLSCAASGYTFSSYWIEWVRQAPGKGLEWIGEILPG
GGDTNYNEIFKGRATFSADTSKNTAYLQMNSLRAEDTAVYYCTRRVPIRLDYWGQGTLVTVSSGGG
GSDIKLQQSGAELARPGASVKMSCKTSGYTFTRYTMHWVKQRPGQGLEWIGYINPSRGYTNYNQK
FKDKATLTTDKSSSTAYMQLSSLTSEDSAVYYCARYYDDHYCLDYWGQGTTLTVSSVEGGSGGSGG
SGGSGGVDDIQLTQSPAIMSASPGEKVTMTCRASSSVSYMNWYQQKSGTSPKRWIYDTSKVASGVP
YRFSGSGSGTSYSLTISSMEAEDAATYYCQQWSSNPLTFGAGTKLELKEQKLISEEDLGSHHHHHH.

2. OKT3-scFv-IgG Fc:

MEAPAQLLFLLLLWLPDTTGMDIKLQQSGAELARPGASVKMSCKTSGYTFTRYTMHWVKQRPGQ
GLEWIGYINPSRGYTNYNQKFKDKATLTTDKSSSTAYMQLSSLTSEDSAVYYCARYYDDHYCLDYW
GQGTTLTVSSVEGGSGGSGGSGGSGGVDDIQLTQSPAIMSASPGEKVTMTCRASSSVSYMNWYQQ
KSGTSPKRWIYDTSKVASGVPYRFSGSGSGTSYSLTISSMEAEDAATYYCQQWSSNPLTFGAGTKLE
LKEQKLISEEDLGSDKTHTCPPCPAPELLGGPSVFLFPPKPKDTLMISRTPEVTCVVVDVSHEDPEVK
FNWYVDGVEVHNAKTKPREEQYNSTYRVVSVLTVLHQDWLNGKEYKCKVSNKALPAPIEKTISKA
KGQPREPQVYTLPPSRDELTKNQVSLTCLVKGFYPSDIAVEWESNGQPENNYKTTPPVLDSDGSFFL
YSKLTVDKSRWQQGNVFSCSVMHEALHNHYTQKSLSLSPGKHHHHHH

3. BV28-scFv-IgG Fc:

MEAPAQLLFLLLLWLPDTTGDIQLTQSPSSLSASVGDRVTITCKASQSVDYEGDSFLNWYQQKPGK

APKLLIYAASNLESGVPSRFSGSGSGTDFTLTISSLQPEDFATYYCQQSNEDPLTFGQGTKVEIKRGGG

GSGGGGSGGGGSEVQLVESGGGLVQPGGSLRLSCAASGYTFSSYWIEWVRQAPGKGLEWIGEILPG

GGDTNYNEIFKGRATFSADTSKNTAYLQMNSLRAEDTAVYYCTRRVPIRLDYWGQGTLVTVSSGGD

KTHTCPPCPAPELLGGPSVFLFPPKPKDTLMISRTPEVTCVVVDVSHEDPEVKFNWYVDGVEVHNA

KTKPREEQYNSTYRVVSVLTVLHQDWLNGKEYKCKVSNKALPAPIEKTISKAKGQPREPQVYTLPP

SRDELTKNQVSLTCLVKGFYPSDIAVEWESNGQPENNYKTTPPVLDSDGSFFLYSKLTVDKSRWQQG

NVFSCSVMHEALHNHYTQKSLSLSPGKHHHHHH